

Nanoplasmonic Multiband Filters Using SIR for Wireless Networks

K. Thirupathaiah, *Member, IEEE*, L. Koteswara Rao, *Member, IEEE*

Abstract— This article demonstrate design and numerical analysis of the multiband band-pass and band-stop filters using an even-mode MIM waveguide-based step impedance resonator (SIR) and simultaneously operated at optical bands O & L bands (185.72 THz and 230.02 THz) with higher efficiency (>35 dB).

I. INTRODUCTION

SURFACE plasmon polaritons (SPPs) are electromagnetic (EM) waves coupled to the oscillations of the conduction electrons at the interface of the metal-dielectric sandwich and propagates with the exponential decaying field in the perpendicular direction to the interface [1]. Conventional waveguides can support only optical signals, whereas SPPs can support both optical and electrical signals. SPPs have distinctive capabilities to carry the energy and information signal due to their overcoming of the conventional diffraction limit, light manipulation at subwavelength scales, reduce the component size into nanometric dimensions, and it is an ideal candidate for high-density PICs. The surface waves are propagating through the metal-dielectric interface with the slow-wave plasma to get the shortest wavelength, minor phase velocity, and major impedance of the surface wave, in contrast to the normal wave in the equivalent dielectric medium. The wave mode is equivalent to transverse electromagnetic (TEM) mode; consequently, the supporting devices have been designed by an equivalent transmission line model.

Several plasmonic filters have been designed like SRRs [2], tooth-shaped filters [3], M-Z interferometer [4], and multiplexers [5]. However, most of these components are not suitable for integration into systems because of their huge size and they can experience a major loss in both bands either in pass band or stop band. They possess more difficulties in making the more compact and efficient next-generation PICs. However, most of these devices suitable only for single-band operation at a time. In this article, we demonstrate the advantage of even mode SIR compared with the odd mode SIR based filters with higher efficiency of more than 35dB return loss [6].

Recently [6], [7], the concurrent dual band band-pass filters and a diplexer has been described in odd mode ($R_Z = Z_2/Z_1 < 1$) case for PICs. The main focus of this article is to design the plasmonic filters for PICs with concurrent dual and operation for pass-band and stop-band filters using by even mode condition ($R_Z = Z_2/Z_1 > 1$). Due to the electric field in even mode condition, the proposed filters have more efficiency (>35dB) in comparison to the previously designed

concurrent dual band filters [6]. The basic properties of the MIM slot waveguide, dual band band-pass filter, and band-stop filter characteristics of SIR have been described. To obtain the numerical solutions of the device, a full-wave analysis solver CST Microwave studio suite has been used.

II. CONCEPT OF THE EVEN MODE SIR

The schematic of plasmonic MIM SIR with and their equivalent transmission line is shown in Fig. 5 with the comparison of [6]. The concept of even and odd mode $\lambda_g/2$ type MIM SIR has been proposed by J.T. Sai Kuo et.al [8]. Resonance occurs in each MIMSIR is either even- or odd-mode and the fundamental resonance happen in the odd-mode case and even-mode case first higher-order resonance will occur and so forth. Thus, the resonance conditions are given by,

$$\tan \theta_1 = R_Z \cot \theta_2 \quad (\text{odd-mode}) \quad (2)$$

$$\tan \theta_2 = -R_Z \tan \theta_1 \quad (\text{even-mode}) \quad (3)$$

where R_Z is the ratio of impedances given by

$$R_Z = Z_2/Z_1 = \tan \theta_1 \tan \theta_2 \quad (4)$$

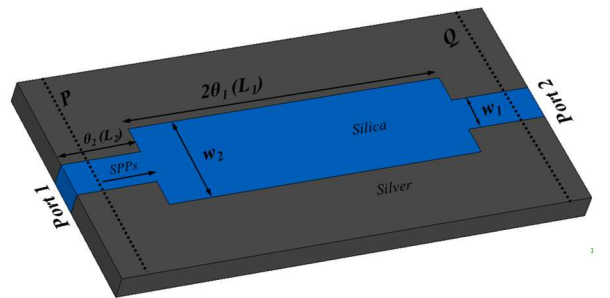


Fig. 1 Geometry of dual band MIMSIR based plasmonic band pass filter for fixed widths $w_1 = 420$ nm, $w_2 = 120$ nm, $L_1 = 2020$ nm, $L_2 = 1010$ nm.

As a result, the resonance condition is dependent on the electrical length of the resonators and also the impedance ratio (R_Z). The equivalent circuits of both even and odd mode MIM SIR are sufficient to support the analysis of near resonance frequencies, and then it is easy to understand the behavior of the circuit at resonance condition. For the special case of $\theta_1 = \theta_3 = \theta_0$, the relationship of the fundamental and spurious resonance frequencies is given by [9];

$$\lambda \frac{f_{S1}}{f_0} = \frac{\pi}{2 \tan^{-1} \sqrt{R_Z}} \quad (5)$$

$$\lambda \frac{f_{S3}}{f_0} = \frac{\pi}{\tan^{-1} \sqrt{R_Z}} \quad (6)$$

where f_0 , f_{S1} and f_{S3} are center, first and second spurious frequencies respectively.

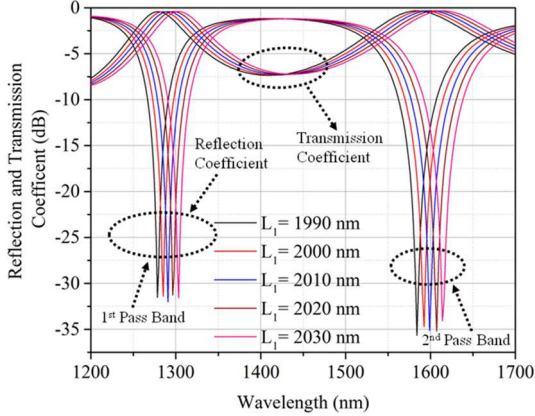


Fig. 2 Variation of transmission and reflection coefficient of with wavelength as a function of length (L_1), $L_2 = 1010$ nm $w_1 = 420$ nm, $w_2 = 120$ nm.

By the concept of even mode SIR as discussed above, band-pass filter characteristics of MIMSIR have been determined by using CST Microwave Studio Suite based upon MIM slot waveguide have shown in Fig. 1. The power monitors P and Q are used to detect the incident and transmitted powers of the filter and kept at a distance of 1522.5nm from the center of the MIMSIR. In the full-wave simulations. The spatial grid along x and y directions are set to be $\Delta x = \Delta y = 5$ nm. The transverse magnetic (TM) mode of the MIM slot waveguide has been started from the left-hand side to the right-hand side of the waveguide. The TM mode can only propagate in the MIM slot waveguide, due to the slot width of the waveguide is much smaller than the guiding wavelength.

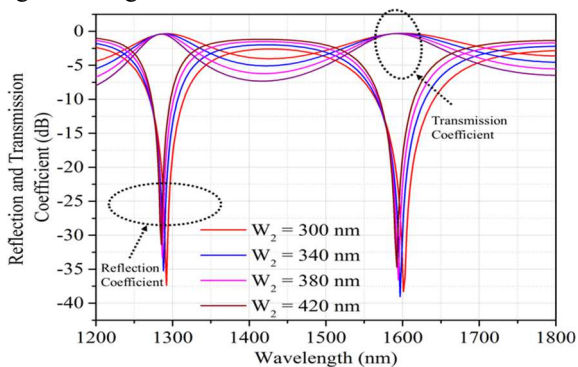


Fig. 3 Variation of reflection and transmission coefficient of with wavelength as a function of length (w_2), $w_2 = 120$ nm, $L_1 = 2020$ nm, $L_2 = 1010$ nm.

Transmission coefficients of the filter are shown in Figs. 2 and 3. Since the object of our design is looking for a band-pass filter with the physical dimensions $w_1 = 420$ nm, $w_2 = 120$ nm, $L_1 = 2020$ nm, $L_2 = 1010$ nm. Using Eq. (5), resonance occurs at $R_Z = 5.8712$ and the first peak of the pass band appear at fundamental frequency $f_0 = 185.72$ THz (1614 nm) simultaneously the second peak of pass band appears at first spurious frequency $f_{S1} = 230.02$ THz (1303 nm) if $\theta_1 = \theta_2 = \theta_0$. However, the second peak of the pass band occurs at

1272 nm in place of 1303 nm as shown in Fig. 6. This kind of shift is possible, due to different electrical lengths θ_1 and θ_2 , when the total electrical length of the resonator ($\theta_T = (\theta_1 + \theta_2)$) is fixed. Fig. 2 and Fig. 3 show the variation in

TABLE I
UNITS FOR MAGNETIC PROPERTIES

W_2 (nm)	λ_{01} (nm)	λ (nm)	$Q =$ λ_{01}/λ	λ_{02} (nm)	λ (nm)	$Q =$ λ_{01}/λ
180	1289	147	9	1596	267	6
200	1295	122	11	1604	218	7
220	1297	107	12	1605	187	9
240	1301	95	14	1610	166	10
260	1304	91	14	1613	150	11

transmission coefficients of the resonator with the parametric changes as a function of L_1 and w_2 . It is clearly shown that the variation in length L_1 offers better impact when it is compared to width w_2 . Table 1 shows the quality factor (Q) of the SIR of two pass bands related to the corresponding Fig.2.

III. CONCLUSION

Using even mode high resonance SIR, concurrent dual band band-pass have been designed and investigated. The designed plasmonic dual band filters operate simultaneously at optical frequency bands (185.72 THz and 230.02 THz) with higher efficiency of more than 35dB. Therefore, the designed plasmonic dual band filters make possible innovative techniques to design nanoscale PICs based on surface plasmon polaritons

REFERENCES

- [1] H. Lu, G. Wang and X. Liu., "Manipulation of light in MIM plasmonic waveguide systems," Chin. Sci. Bull., Vol. 58, no. 30, pp. 3607-3616, Oct. 2013.
- [2] J. Wen, J. Chen, K. Wang, B. Dai, Y. Huang and D. Zhang, "Broadband plasmonic logic input sources constructed with dual square ring resonators and dual waveguides," IEEE Photonics J., vol. 8, no. 2, pp. 1-9, Apr. 2016.
- [3] Xian-Shi Lin and Xu-Guang Huang, "Tooth-shaped plasmonic waveguide filters with nanometric sizes," Opt. Lett., vol. 33, no. 23, pp. 2874-2876, Dec. 2008.
- [4] J. Gosciniaik, L. Markey, A. Dereux, and S. I. Bozhevolnyi, "Thermo-optic control of dielectric-loaded plasmonic Mach-Zehnder interferometers and directional coupler switches," Nanotechnology, vol. 23, no. 44, pp. 444008 (1-9), Oct. 2012.
- [5] V. Liu, Y. Jiao, D. A. B. Miller, and S. Fan, "Design methodology for compact photonic-crystal-based wavelength division multiplexers," Opt. Lett., vol. 36, no. 4, pp. 591-593, Feb. 2011.
- [6] K. Thirupathaiiah, S. Member, N. P. Pathak, and V. Rastogi, "Concurrent Dual Band Filters Using Plasmonic Slot Waveguide," IEEE Phot. Tech. Lett., vol. 25, no. 22, pp. 2217-2220, Nov. 2013.
- [7] K. Thirupathaiiah, B. Iyer, N. Prasad Pathak, and V. Rastogi, "Concurrent dualband diplexer for nanoscale wireless links," IEEE Photonics Technol. Lett., vol. 26, no. 18, pp. 1832-1835, Sep. 2014.
- [8] J.T. Kuo, T.H. Yeh, and C.C. Yeh, "Design of microstrip bandpass filters with a dual-passband response," Microw. Theory Tech. IEEE Trans., vol. 53, no. 4, pp. 1331-1337, Apr. 2005.
- [9] M. Makimoto S. Yamashita, "Microwave Resonators and Filters for Wireless Communication," Springer-Verlag Berlin Heidelberg, 4th Edition.